
Quantitative and Clinical Analysis of SPECT Image Registration for Epilepsy Studies

Benjamin H. Brinkmann, Terence J. O'Brien, Shmuel Aharon, Michael K. O'Connor, Brian P. Mullan, Dennis P. Hanson and Richard A. Robb

Biomedical Imaging Resource, Departments of Neurology and Nuclear Medicine, Mayo Foundation, Rochester, Minnesota; and Imaging and Visualization, Siemens Corporate Research, Princeton, New Jersey

This study reports quantitative measurements of the accuracy of two popular voxel-based registration algorithms—Woods' automated image registration algorithm and mutual information correlation—and compares these with conventional surface matching (SM) registration. **Methods:** The registration algorithms were compared (15 different matches each) for (a) three-dimensional brain phantom images, (b) an ictal SPECT image from a patient with partial epilepsy matched to itself after modification to simulate changes in the cerebral blood flow pattern and (c) ictal/interictal SPECT images from 15 patients with partial epilepsy. Blinded visual ranking and localization of the subtraction images derived from the patient images were also performed. **Results:** Both voxel-based registration methods were more accurate than SM registration ($P < 0.0005$). Automated image registration algorithm was more accurate than mutual information correlation for the computer-simulated ictal/interictal images and the patient ictal/interictal studies ($P < 0.05$). The subtraction SPECTs from SM were poorer in visual ranking more often than the voxel-based methods ($P < 0.05$). **Conclusion:** Voxel intensity-based registration algorithms provide significant improvement in ictal/interictal SPECT registration accuracy and result in a clinically detectable improvement in the subtraction SPECT images.

Key Words: image registration; ictal/interictal SPECT; partial epilepsy; cerebral blood flow

J Nucl Med 1999; 40:1098–1105

Several computer-aided methods for producing subtraction ictal SPECT images coregistered to MRI (SISCOM) have recently been described as tools for improving the localization of the epileptogenic zone in focal epilepsy (1–4). These methods have been shown to significantly improve sensitivity and specificity compared with conventional visual analysis of ictal/interictal SPECT images (3,5,6). The SISCOM methods involve acquiring both ictal and interictal SPECT images of regional cerebral blood flow (rCBF) using a radiolabeled tracer, usually ^{99m}Tc hexamethylpropylene amine oxime or ^{99m}Tc -ethyl cysteinyl diethyl-ester (ECD). These functional rCBF maps are then normal-

ized to mean cerebral pixel intensity to account for differences in total activity and isotope decay, registered using an accurate and robust matching algorithm to account for differences in patient position and slice level and subtracted to produce a functional map of the changes in rCBF during ictus compared with the resting state. This subtraction image is then thresholded to isolate significant blood flow changes and is registered to the patient's MR image.

One of the major influences on the sensitivity and specificity of the SPECT subtraction image is the accuracy of the ictal/interictal SPECT image alignment (1). Poor registration results in subtraction of nonanatomically corresponding voxels. This decreases the sensitivity of the final image by increasing the signal-to-noise ratio and may decrease specificity by producing false-positive activation sites. Brain surface matching techniques (7,8) have traditionally been used to produce subtraction SPECT images (1,2). Surface matching (SM) coregistration consistently matches SPECT images with better than 1 voxel dimension of accuracy (1); however, the literature suggests that even small misalignments may decrease the sensitivity of focal uptake detection (9). Hence, methods that provide more accurate interictal-to-ictal SPECT registration have the potential to further improve the sensitivity and specificity of epileptogenic localization.

The SM algorithm we originally used in SISCOM was developed by Jiang et al. (8) in 1992 and is available as part of the AnalyzeAVW software package (Mayo Foundation, Rochester, MN) (10). This algorithm has been extensively used by many centers and has been demonstrated to be robust and accurate for several different imaging modalities (11–13). Recently, several voxel-based registration algorithms have been proposed for inter- and intramodality image alignment, and these methods have been shown to be even more accurate than SM methods for a variety of applications (11). However, the performance of different algorithms depends greatly on the image modalities used and the registration task to be performed, and few have been compared quantitatively for matching functional rCBF images. In particular, the extensive changes in image contrast that accompany ictal activation could confound voxel-based registration algorithms. Most intramodality voxel-based algorithms depend on a certain consistency of voxel gray

Received Jul. 20, 1998; revision accepted Oct. 22, 1998.

For correspondence or reprints contact: Richard A. Robb, PhD, Director, Biomedical Imaging Resource, Medical Sciences 2–135, Mayo Foundation, Rochester, MN 55905.

values between images, whereas most voxel-based intermodality algorithms assume that a given gray value range in one image reliably maps to a different gray value range in the other image. Neither of these assumptions are necessarily true in matching peri-ictal and interictal SPECT images, as rCBF and hence image contrast can change drastically and unpredictably between images. It has been suggested that SM may actually be preferable to other methods for ictal/interictal SPECT coregistration because the cortical surface shape is independent of changes in the rCBF between the two images (1).

Previous registration validation studies have generally focused on PET-to-PET imaging and intermodality image registration (11,14–16). Although some generalizations may be formed from these studies, the lower resolution of SPECT images compared with PET and the marked rCBF and image contrast changes between ictal and interictal SPECT images require an explicit validation of the coregistration methods for this application. The purpose of this study was to quantitatively compare the interictal-to-ictal SPECT registration accuracy of traditional SM with two leading voxel-based image registration algorithms, Woods' automated image registration (AIR 3.0) and mutual information (MI) (16–19).

MATERIALS AND METHODS

Registration Algorithms

Each registration algorithm has different parameters, which may be altered to optimize the registration for a particular task, and the use of suboptimal parameters would be expected to affect registration results noticeably. For each algorithm used in this study, parameters were selected to give greatest accuracy without concern for processing time. Most voxel intensity-based registration algorithms offer the option to calculate the algorithm's cost function from a subsampled group of image voxels during preliminary iterations. Parameters were verified, and the degree of subsampling used was determined by testing each algorithm on several test cases. All algorithms used a six-parameter linear model, and no initial alignment guesses were used.

Surface Matching

The brain SM algorithm used was that described by Jiang et al. (8) in 1992, which is available as part of the AnalyzeAVW software package (10). This algorithm uses a multiresolution gradient descent approach to minimize the chamfer distance between two surfaces that must be defined a priori by the user. Two binary images representing the cerebral surface for each scan are created by thresholding above the value for extracerebral uptake (supplemented if necessary by manual deletion), followed by two-dimensional morphologic processing for hole deletion. The algorithm samples 1000 points on the surface of the first cerebral binary image and matches these points to the corresponding three-dimensional surface of the other cerebral binary image. A 4×4 homogeneous transformation matrix is returned that describes the best-fit three-dimensional transformation. A previous study had demonstrated that this method produced a "worst case" coregistration error of less than 1 voxel diameter for 15 successive matches of a three-dimensional brain phantom (median 3.2 mm, range 1.2–4.8 mm) (1). A similar value was found for the root mean square

distance error between corresponding points on registered interictal-to-ictal SPECTs from 10 consecutive patients with intractable partial epilepsy (median 2.2 mm, range 1.6–2.9 mm) (1).

Mutual Information

Matching by maximization of mutual information was proposed and developed by Studholme et al. (16) and Wells et al. (19). The algorithm has performed well in several intermodality tasks (11,16,19), but to our knowledge has never been evaluated for ictal/interictal SPECT applications. The specific implementation of MI we used (20) is available in the AnalyzeAVW software package (10) and uses the simplex method to maximize the mutual information of the two images, which in turn depends primarily on minimizing the joint entropy of the two images. Image entropy is a measure of disorder or uncertainty, so this process can be thought of as maximizing the propensity of pixel values in one image to be predictive of the value of the corresponding pixels in the other image. Typical parameters were used, including parameter tolerance of 1×10^{-8} , function tolerance of 0.001, 1000 iterations per step, and 1:1 voxel sampling (i.e., no subsampling was used) for all steps.

Automated Image Registration

The AIR algorithm aligns two images by first thresholding to remove background noise and then using a Newton-Raphson method to minimize the SD of the ratio of corresponding image gray values (17,18). In a previous multicenter study, AIR performed the best of the three algorithms for intermodality registration tasks (11), although only slightly better than MI algorithms. For our studies, we used AIR 3.0, obtained from University of California-Los Angeles. The images were matched using the intramodality registration settings. Typical parameters were used, including convergence change threshold of 0.00001 and initial sampling of 81:1 with a factor of 3 decrement at each step. Unlike the MI algorithm, test case results were better with incremental subsampling than with 1:1 sampling. The same thresholds were used for AIR as were used in the SM algorithm. No smoothing kernel was used, as our images were smoothed already during reconstruction.

Brain Phantom Images

Six sequential scans of a realistic three-dimensional volumetric brain phantom (Hoffman 3D brain phantom; Data Spectrum Corp., Hillsborough, NC) containing 555 MBq (15 mCi) ^{99m}Tc were taken, rotating the phantom in the headrest about the central axis of the scanner for each scan. A digital spirit level (Pro Smart Level; Wedge Innovations, San Jose, CA) was taped to the phantom, and images were acquired at rotations of 0.0°, 1.5°, 3.0°, 5.0°, 10.0° and 14.9°. Images were acquired at 140 keV with a 20% window in 120 views at 3° increments on a dual-head gamma camera system with fanbeam collimators at a minimum radius of rotation. Because of the high ^{99m}Tc activity in the phantom, acquisition time was limited to 10 s per frame. The images were reconstructed on a 64×64 grid, with cubic voxel dimensions of 4.4 mm per side (Fig. 1), using a standard filtered backprojection algorithm and a third-order Metz filter (6 mm full width at half maximum). To provide a more challenging registration task using 4 degrees of freedom, the reconstructed images were then misaligned by known amounts. Net misalignments are listed in Table 1. Each scan was then registered to the other 5 scans, creating 15 registration tasks to be evaluated. Reference 4×4 transformation matrices were constructed using the known rotation and translation parameters, and these matrices

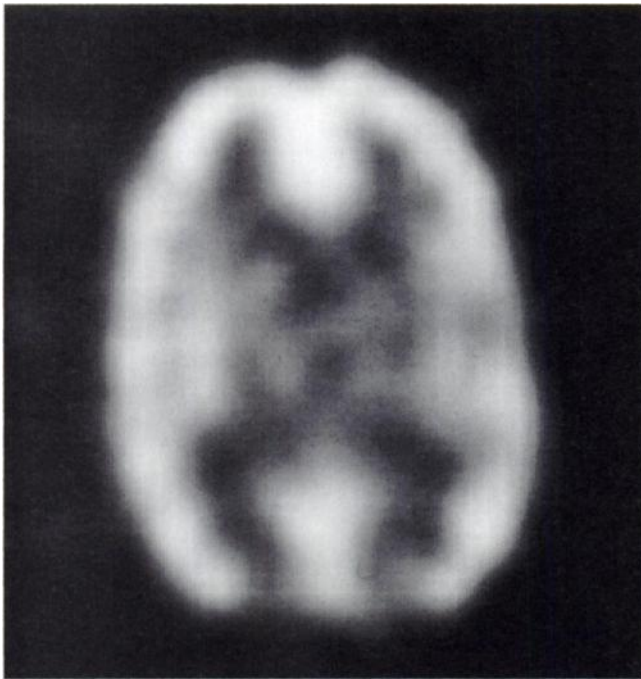


FIGURE 1. Transverse slice through brain phantom SPECT image.

were inverted and multiplied by the matrices given by the registration algorithms to give a residual error matrix. These matrices were evaluated for a point on the phantom's surface at the maximum distance from the center of rotation, at 79.3 mm. This represents the worst case misregistration (in millimeters) for cortical gray matter voxels and is the same method reported in the original validation of the SM SPECT-to-SPECT coregistration for SISCOM studies (1).

Patient Ictal/Interictal Simulation

Although phantom images can approximate patient SPECT scans and allow for reliable, quantitative estimates of registration accuracy, phantoms cannot adequately model the dramatic changes that can occur in the pattern of rCBF between ictal and interictal images. However, when registering patient images, the true registration is never known. To measure registration accuracy, it would be ideal to obtain a pair of images that are misregistered by a known transformation and that display similar intensity changes to those

seen between ictal and interictal SPECT images. In an attempt to simulate this we obtained a true ictal patient image (patient 2) and manually replaced apparent focal activation sites with the mean cerebral pixel intensity, and then systematically modified the contrast in various parts of the image by adding areas of increased and decreased rCBF (bright and dark pixels, respectively) over areas of average intensity. We also added a large area of very bright pixels (mean cerebral pixel intensity plus 4 SD) along the superior left cortex and a small area near the basal nuclei to further alter the image contrast. These activation sites are greater than normally found in patient scans, and hence the simulation represents a worst case scenario for ictal-interictal images. The image was blurred in the transverse plane with a 3×3 mean filter, and zero-mean Gaussian noise ($\pm 18\%$ of mean cerebral pixel count) was added. The resulting image had very different contrast (and hence rCBF patterns) and reduced resolution compared with the patient's ictal image, but had identical shape and was in perfect coregistration to it (Fig. 2). The registration comparison experiment was then repeated using the real ictal and simulated patient images. The rotations and translations listed in Table 1 were applied to both the real and simulated images. Fifteen matches were performed for each of the three registration algorithms, using the real image as the base volume and the simulated image as the match volume in each experiment.

Patient Ictal/Interictal SPECT Registrations

Fifteen consecutive patients with partial epilepsy were studied. Each had ictal and interictal SPECT imaging performed as part of their presurgical evaluations, according to a standard clinical protocol (5). Of the 15 patients, 4 had temporal lobe epilepsy and 11 had extratemporal lobe epilepsy. Images were acquired at a minimum radius of rotation on a dual-head gamma camera system equipped with fanbeam collimators. A total of 120 views were taken at 3° increments at 15 s per frame using a 20% window at 140 keV. Filtered backprojection reconstruction was performed with a third-order Metz smoothing filter, usually on a 64×64 grid. Ictal injections of 740 MBq (20 mCi) ^{99m}Tc -ECD were administered by trained technologists in the epilepsy monitoring unit after the first indication of abnormal behavior or impaired awareness. Interictal injections of 740 MBq (20 mCi) ^{99m}Tc -ECD were given in ambient room lighting with eyes open and ears unplugged after at least 24 seizure-free h. Images were acquired within 2 h of isotope injection.

TABLE 1
Six Brain Phantom Images and Misregistrations
Applied to Them

Image	x-rotation	y-rotation	z-rotation	z-translation
1	0.0	0.0	0.0	0.0
2	-14.9	-14.9	1.5	-2.5
3	-10.0	-10.0	3.0	-2.0
4	-5.0	-5.0	5.0	-1.5
5	-3.0	-3.0	10.0	-1.0
6	-1.5	-1.5	14.9	-0.5

Rotations are given in degrees, while translations are given in voxel units, equal to 4.4 mm. Rotations were applied and evaluated assuming a z-y-x rotation order.

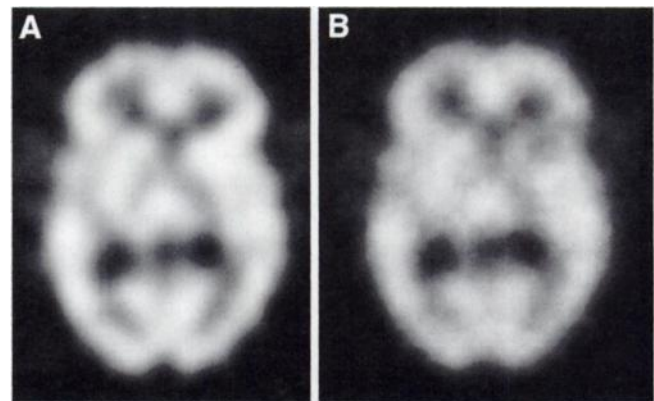


FIGURE 2. Transverse slice through ictal SPECT image from patient 2 (A) and corresponding slice from contrast-altered simulation image (B).

As the true positions of the ictal and interictal images in each patient could not be known, an absolute measure of registration accuracy could not be obtained in these patients. As a surrogate measure of accuracy, the SDs of nonzero (cerebral) pixels in their resultant subtraction images were compared. The subtraction images were formed by normalizing the ictal and interictal SPECT images to mean cerebral pixel counts, applying a user-chosen threshold to isolate cerebral cortex voxels, filling the ventricles using math morphology and subtracting only the overlapping nonzero voxels as previously described (1). If the two scans were in perfect alignment, the SD of nonzero pixels in the subtraction image would be expected to be minimized.

To validate this as a metric for registration accuracy, we plotted the effect on the subtraction image SD of applying several known misalignments to pairs of SPECT images of two different types: (a) two phantom SPECTs that were initially aligned by applying a computer-aided rotation in the z-axis to the second SPECT to compensate for the difference between the phantom positions that had been measured with the digital spirit level during their acquisition and (b) the ictal and interictal SPECT images from patient 2 that were aligned using the AIR algorithm. For each experiment, the match image was misregistered by a known, constant amount, and the SD of the subtraction image was calculated.

Blinded Visual Comparison

A blinded visual comparison of the different subtraction SPECT images derived from each of the three registration methods was performed for the 15 patients to determine whether the voxel-based registration methods consistently produced visually detectable improvement in the SISCOM subtraction images. For each patient, three thresholded subtraction SPECT images (created with each of the three registration algorithms) were presented in a random order to a single reviewer who was experienced in reading both SISCOM and traditional side-by-side ictal and interictal SPECT images. The reviewer, who was blinded to each patient's clinical details and the registration method used, was asked to rank the quality of the three subtraction images according to (a) their clarity in localizing an apparent epileptogenic focus and (b) the amount of background noise, particularly around ventricles or in white matter areas. The thresholded subtraction images were overlaid onto the patient's ictal SPECT and MR image (if available) to provide visual context for the images, and both sets of composite images were made available to the reviewer. The reviewer was not permitted to rank any images as being equal in quality.

Blinded Visual Localization

An additional blinded study was performed on images from the same 15 patients to determine whether the misregistrations observed in this study could affect the clinical localization. The thresholded subtraction SPECT images derived from each of the three registration methods (45 images in total) were presented in a random order to the same reviewer, who was blinded to patient identity, the clinical details and the registration method used. The reviewer rated each SISCOM image as localizing, lateralizing or nonlocalizing. If the images were rated as localizing, 1 of 18 possible epileptogenic localizations was chosen (i.e., frontal, frontotemporal, temporal, frontoparietal, temporo-parietal, temporo-occipital, parietal, parietooccipital or occipital). These localizations were then compared with one another and with the clinical discharge diagnosis (i.e., the diagnosis rendered by the attending physician on discharge from the epilepsy monitoring unit, based on

the clinical features, the video-electroencephalogram findings and the MR image).

Statistical Methods

Statistical analysis was performed with the aid of a commercially available statistical package (STATISTICA 4.5 for Windows; Statsoft, Inc., Tulsa, OK). For each type of SPECT image (i.e., phantom, simulated ictal/interictal and patient ictal/interictal), accuracy of the three types of registration methods was compared for the same 15 matches using analysis of variance (ANOVA) for repeated measures. Testing for planned comparisons was also performed between the two voxel matching methods. Friedman ANOVA by ranks was used to compare the visual ranking of the quality of the subtraction images derived by the three different registration methods in the 15 patients with partial seizure. The level for statistical significance was set at $P < 0.05$ for all tests.

RESULTS

Brain Phantom Images

Registration results for 15 different matches from the six brain phantom SPECT images are shown in Table 2. ANOVA for repeated measures demonstrated that the registration errors were significantly greater for the SM than for either of the voxel-based methods ($P < 0.0005$). The planned comparison analysis demonstrated no significant differences between errors for the MI and AIR algorithms.

Patient Ictal/Interictal Simulation Images

Table 3 lists results from the 15 matches using the simulated patient SPECT as the match volume and the real ictal image as the base. ANOVA results show that SM had significantly larger registration errors than either of the

TABLE 2
Fifteen Brain Phantom Matches Reported as Total Error*

Base	Match	Surface (mm)	Mutual information (mm)	AIR (mm)
1	2	4.25	1.89	1.28
1	3	2.32	1.66	1.70
1	4	2.40	1.68	2.10
1	5	3.87	2.19	2.58
1	6	2.04	2.48	2.91
2	3	1.14	0.70	0.95
2	4	1.09	1.28	1.86
2	5	3.50	1.71	1.60
2	6	4.23	2.73	1.84
3	4	2.53	1.30	1.39
3	5	3.73	2.16	4.95
3	6	4.47	3.20	2.51
4	5	4.12	1.50	1.31
4	6	2.38	2.26	1.93
5	6	4.15	0.89	0.77
Mean error		3.08†	1.84	1.98

*Calculated for a point on the surface of the brain phantom at maximal distance from the center of rotation.

†Surface matching errors significantly greater than either voxel matching methods ($P < 0.0005$, ANOVA for repeated measures).

AIR = automated image registration.

TABLE 3
Fifteen Patient Brain Ictal/Interictal SPECT Simulation
Matches Reported as Total Error

Base	Match	Surface (mm)	Mutual information (mm)	AIR (mm)
1	2	2.17	0.71	0.22
1	3	2.07	0.51	0.29
1	4	2.68	0.03	0.33
1	5	1.77	0.36	0.41
1	6	1.75	0.76	0.68
2	3	3.62	0.13	0.34
2	4	4.38	2.55	0.69
2	5	3.76	1.35	0.80
2	6	4.54	2.57	1.77
3	4	0.30	0.16	0.28
3	5	0.73	0.79	0.29
3	6	2.35	1.61	0.90
4	5	1.89	0.47	0.44
4	6	3.10	0.79	0.31
5	6	2.28	0.35	0.42
Mean error		2.49*	0.88†	0.54†

*Surface matching errors significantly greater than either voxel matching methods ($P < 0.0005$, ANOVA for repeated measures).

†Errors for mutual information significantly greater than for AIR ($P < 0.05$, ANOVA for repeated measures).

AIR = automated image registration.

TABLE 4
Standard Deviation of Nonzero Pixels in Ictal/Interictal
Subtraction Image for 15 Patients with Epilepsy

Patient no.	Surface	Mutual information	AIR
1	13.129	12.447	11.822
2	13.340	11.969	11.849
3	11.540	10.659	10.551
4	11.253	10.010	9.821
5	13.301	11.608	11.017
6	14.771	14.588	14.369
7	11.493	11.333	11.139
8	11.197	11.016	10.918
9	13.049	11.757	11.559
10	12.948	13.269	11.277
11	11.543	11.487	11.340
12	11.648	9.924	9.802
13	11.041	10.375	10.381
14	11.854	9.847	9.568
15	10.628	10.345	9.299
Mean error	12.18*	11.38†	10.98†

*Surface matching errors significantly greater than either voxel matching methods ($P < 0.0005$, ANOVA for repeated measures).

†Errors for mutual information significantly greater than for AIR ($P < 0.05$, ANOVA for repeated measures).

AIR = automated image registration.

voxel-based methods ($P < 0.0001$). However, on this occasion the planned comparison analysis showed that the matching errors were significantly less for AIR than for MI ($P < 0.05$).

Patient Ictal/Interictal Images

Figure 3 shows the SD of the subtraction images plotted against total known misregistration error for the phantom and patient images. This demonstrates that the SD progressively increases as registration error increases, particularly beyond half a voxel dimension in misregistration. Table 4 lists SDs of subtraction images for each of the 15 patients

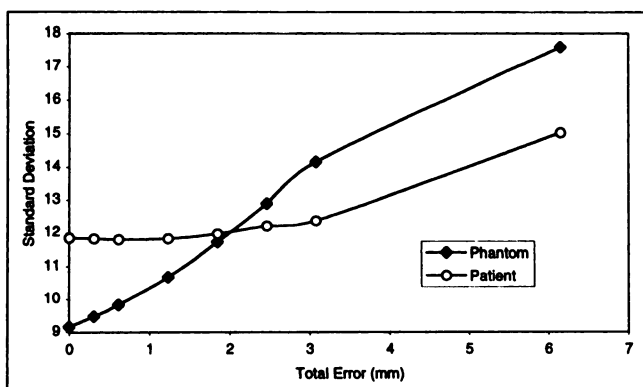


FIGURE 3. SD of SISCOM subtraction image plotted versus misregistration total error for two phantom images, and for ictal and interictal images for patient 2. For patient images, match generated by AIR algorithm was taken as "true" coregistration.

derived using the three different ictal/interictal SPECT registration methods. ANOVA for repeated measures demonstrated that the SDs of the subtraction images were significantly higher for the SM method than for the voxel-based algorithms ($P < 0.0001$). A planned comparison analysis also demonstrated that AIR produced subtraction images with a significantly lower SD than MI ($P < 0.05$).

Blinded Visual Comparison

The results of the blinded visual ranking of the quality of the subtraction SPECT images for the 15 partial seizure patients are shown in Table 5. The subtraction SPECT images from SM were ranked significantly worse than those from either of the two voxel-matching methods ($P < 0.05$).

TABLE 5
Frequency of Best, Second and Worst Visual Ranking
of Quality of Subtraction SPECT Images for Three
Different Registration Methods

	Surface	Mutual information	AIR
Best	3*	4	8
Second	1*	9	5
Worst	11*	2	2

*Surface matching was ranked significantly poorer than the other two methods ($P < 0.05$, Friedman ANOVA by ranks).

AIR = automated image registration.

There were no statistically significant differences between the AIR and MI subtraction image rankings.

Blinded Visual Localization

The results from the blinded visual epileptogenic localizations from the thresholded SPECT subtraction images created using the SM, MI and AIR algorithms are shown in Table 6. The two voxel-based algorithms were concordant with one another in 93% of the images, whereas surface matching was concordant with voxel matching in only 60% of cases. The blinded visual SISCOM localization showed a high concordance with the discharge diagnosis for all three matching methods, but in 1 patient the SM SISCOM image was not concordant with the discharge diagnosis, whereas both voxel-matching methods were.

DISCUSSION

The greatest difficulty in estimating the error in ictal-interictal SPECT registration arises because the true registration between patient images is never known, and a completely objective measure of accuracy cannot be applied. The SISCOM subtraction image SD is certainly not a perfect measure of accuracy. The SD of the ratio image, minimized by the AIR algorithm, is related to the SISCOM SD and may potentially create a bias in favor of the AIR algorithm. Hence the data in Table 4 must be viewed in the context of the validation data presented in Figure 3, as well as the blinded clinical ranking and epileptogenic localization studies. It is the convergence of these tests toward voxel matching and the AIR algorithm that is convincing, rather than just the SD data in Table 4 alone.

Figure 3 illustrates the uniqueness of the ictal/interictal coregistration problem and the effects that large changes in rCBF have on image metrics. Although the homogeneous phantom image experiment shows a mostly linear trend of SD versus total misregistration error, the patient ictal/interictal image curve flattens out near zero, particularly when the registration error is less than half a voxel in size. Three factors contributed to this effect. First, there may be some residual misregistration between the two images.

Second, the trilinear interpolation in the transformation of the second image smoothes the image by varying amounts as the misregistration approaches a half voxel in translation or 45° of rotation. Images with small total misregistration errors are smoothed less by the interpolation algorithm, leaving more noise in the image and thereby increasing the SD of the subtraction image. This is unlikely to represent a significant problem in clinical situations, where the initial misalignment of the ictal and interictal images would almost always be more than half a voxel in size. Third, the SISCOM subtraction SD ignores the contribution from the outer edges of the brain, enhancing the relative contribution to the SD by focal activation sites and rCBF changes to the SD. Thus, when two images near perfect alignment, focal activation sites are sharper and more intense in the subtraction image. This prevents the existence of a sharp minimum in the SISCOM SD, but it also represents an improvement in the sensitivity of SISCOM epileptogenic localization.

There is a great deal of intersubject variability in the magnitude and extent of the changes in rCBF between ictal and interictal SPECT images in partial epilepsy patients. Therefore, the ideal registration algorithm for subtraction ictal SPECT studies should be accurate across the spectrum of rCBF changes. The experiments reported in this article test SPECT-to-SPECT coregistration accuracy across the gamut of rCBF conditions, from cases with very little focal activation (the phantom experiments) to a case with very intense rCBF changes (the patient simulation images), with the patient studies falling somewhere in between. The voxel intensity-based coregistration methods examined in this study are clearly superior to surface-based registration for all three types of SPECT images.

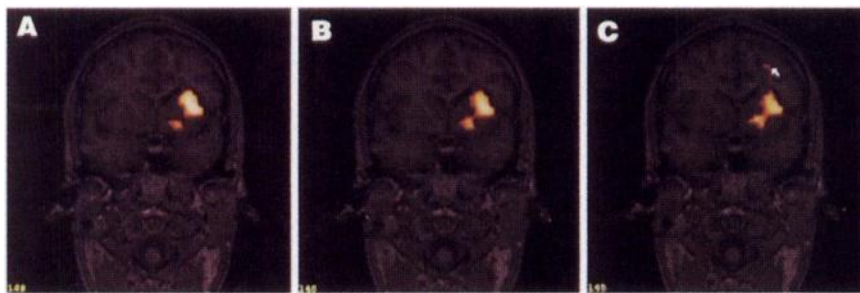
The simulation experiments and patient data experiments suggest that the MI cost function may be hampered by changes in rCBF more so than the AIR cost function. Either of these algorithms would be expected to give excellent results for SISCOM, although the use of AIR may improve the subtraction image slightly. The AIR cost function tends to reduce variation in the ratio image, which should be dominated by sharp image intensity transitions around the ventricles and near image edges. In contrast, the MI cost function tends to align images so that pixel values in one image are maximally predictive of pixel values in the other, which does not necessarily hold true for the large contrast changes between ictal and interictal SPECT images. There is a nonstatistically significant trend in favor of MI for our phantom images, which have mostly static contrast, suggesting that MI may be more accurate than AIR for static contrast anatomic image matching. However, AIR is more robust to functional rCBF-related contrast changes than MI, and there is a trend in the visual rankings suggesting that the improved registration accuracy with AIR may be clinically significant compared with MI. Because the success of the SISCOM epileptogenic localization depends on many factors in addition to the accuracy of the registration algorithm,

TABLE 6
Blinded SISCOM Localization

	SM	MI	AIR
Number (percent)			
localizing	12 (80.0%)	13 (86.7%)	14 (93.3%)
Agreement with SM	—	9 (60%)	10 (66.7%)
Agreement with MI	9 (60%)	—	14 (93.3%)
Agreement with AIR	10 (66.7%)	14 (93.3%)	—
Concordance with epilepsy diagnosis*	10/12 (83.3%)	10/12 (83.3%)	11/13 (84.6%)

*When both the blinded SISCOM interpretation and the epilepsy diagnosis were localizing.
AIR = automated image registration; SM = surface matching; MI = mutual information.

FIGURE 4. With increasing ictal/interictal misregistration, there is reduction in intensity and increase in size of focal activation region, as well as appearance of false-positive activation region (arrow). (A) alignment, (B) 0.28 voxel misalignment and (C) 0.70 voxel misalignment. (Subtraction images were created with AIR registration and were thresholded at same intensity value.)



(for example, injection timing and SPECT image quality) (5), the dominance of the voxel-based methods would not be expected to be as striking in this data (Table 6). However, it is noteworthy that for one of our 15 patients, the improved accuracy afforded by the voxel-based methods compared with SM did make the difference between a localization that was concordant with the discharge diagnosis and one that was not.

It has been suggested that misregistrations on the order of an eighth voxel in translation or 1° of rotation can degrade focal spot intensity by 5%–10% (9) and hence could degrade SISCOM sensitivity. The data from our patient ictal/interictal misregistration study shows that errors greater than half a voxel result in a dramatic rise in the SD of the subtraction image. Figure 4 illustrates the effect of interictal to ictal SPECT misregistration on the final SISCOM image. As the two images were increasingly misaligned, the focal activation site became less intense and larger, and a “false-positive” activation site began to appear, even though all the registration errors were less than one voxel in size. In our experiments, the SM algorithm had many matches that were larger than this value, suggesting that the improved accuracy with voxel-matching registration algorithms should result in a noticeable improvement in the final SISCOM image. This is supported by the results of the blinded visual ranking for the 15 patients with partial seizure (Table 5). Previous clinical studies have shown that SISCOM images constructed using SM consistently and accurately localize the epileptogenic zone in patients with intractible partial epilepsy (5,21). The increased registration accuracy obtained using voxel matching may further improve the clinical accuracy and reliability of SISCOM, but comprehensive clinical studies are necessary to determine this conclusively.

CONCLUSION

The results of this study have demonstrated that voxel-based registration is significantly more accurate than surface-based registration for SPECT-to-SPECT coregistration. These results also demonstrated that Woods' AIR algorithm is more robust to changes in rCBF than MI matching, and therefore may be more appropriate for use in deriving subtraction SPECT images from ictal and interictal images in patients with partial epilepsy. It has also been demonstrated that SPECT-to-SPECT misregistration, particularly when greater than half a voxel in magnitude, decreases the quality of the subtraction SPECT image, potentially decreasing the sensi-

tivity and specificity of SISCOM in the localization of the epileptogenic zone in patients with partial epilepsy. Use of the voxel-based registration algorithms resulted in a clinically detectable improvement in the quality of the final subtraction SPECT image compared with SM.

ACKNOWLEDGMENTS

We acknowledge David R. Holmes III and Dr. Roger P. Woods for their assistance and helpful discussions. We further acknowledge Dr. Woods for use of the AIR 3.0 software. Some software and computer support for this project was funded indirectly through AnalyzeAVW software royalties.

REFERENCES

- O'Brien TJ, O'Connor MK, Mullan BP, et al. Subtraction ictal SPECT co-registered to MRI in partial epilepsy: description and technical validation of the method with phantom and patient studies. *Nucl Med Commun.* 1998;19:31–45.
- Zubal IG, Spencer SS, Imam K, Smith EO, Wisniewski G, Hoffer PB. Difference images calculated from ictal and interictal technetium-99m-HMPAO SPECT scans of epilepsy. *J Nucl Med.* 1995;36:684–689.
- Weder B, Oettli R, Maguire RP, Vonesch T. Partial epileptic seizure with versive movements examined by [^{99m}Tc]HMPAO brain single photon emission computed tomography: an early postictal case study analyzed by computerized brain atlas methods. *Epilepsia.* 1996;37:68–75.
- Chiron C, Jaminska A, Cieuta C, Vera P, Plouin P, Dulac O. Ictal and interictal subtraction ECD-SPECT in refractory childhood epilepsy. *Epilepsia.* 1997;38(suppl 3):9.
- O'Brien TJ, So EL, Mullan BP, et al. Subtraction ictal SPECT co-registered to MRI improves clinical usefulness of SPECT in localizing the surgical seizure focus. *Neurology.* 1998;50:445–454.
- Zubal G, Spanaki-Varelas M, MacMullan J, Spencer SS. Quantitative evaluation of postictal SPECT for seizure localization [abstract]. *Epilepsia.* 1997;38(suppl 8):52.
- Pelizzari CA, Chen GTY, Spelbring DR, Weichselbaum RR, Chen CT. Accurate three-dimensional registration of CT, PET, and/or MRI images of the brain. *J Comput Assist Tomogr.* 1989;13:20–26.
- Jiang H, Robb RA, Holton KS. A new approach to 3-D registration of multimodality medical images by surface matching. *Visualization in Biomedical Computing 1992 Proceeding.* 1992;1808:196–213.
- Sychra JJ, Pavel DG, Chen Y, Jani A. The accuracy of SPECT brain activation images: propagation of registration errors. *Med Phys.* 1994;21:1927–1932.
- Hanson DP, Robb RA, Aharon S, et al. New software toolkits for comprehensive visualization and analysis of three-dimensional multimodal biomedical images. *J Digital Imaging.* 1997;10:31–35.
- West J, Fitzpatrick JM, Wang MY, et al. Comparison and evaluation of retrospective intermodality brain image registration techniques. *J Comput Assist Tomogr.* 1997;21:554–566.
- Brinkmann BH, O'Brien TJ, Dresner MA, Sharbrough FW, Lagerlund TD, Robb RA. Accuracy of scalp-recorded EEG localization on MRI volume data. *Brain Topography.* 1998;10:245–253.
- Hogan RE, Cook MJ, Kilpatrick CJ, Binns DW, Desmond PM, Morris K. Accuracy of coregistration of single-photon emission CT with MR via a brain surface matching technique. *AJNR* 1996;17:793–797.

14. Kiebel SJ, Ashburner J, Poline J-P, Friston KJ. MRI and PET coregistration: a crossvalidation of SPM and AIR. *Neuroimage*. 1997;5:271-279.
15. Strother SC, Anderson JR, Xu X-L, Liow J-S, Bonar DC, Rottenberg DR. Quantitative comparisons of image registration techniques based on high resolution MRI of the brain. *J Comput Assist Tomogr*. 1994;19:117-124.
16. Studholme C, Hill DLG, Hawkes DJ. Automated three-dimensional registration of magnetic resonance and positron emission tomography brain images by multiresolution optimization of voxel similarity measures. *Med Phys*. 1997;24:25-35.
17. Woods RP, Cherry SR, Mazziotta JC. Rapid automated algorithm for aligning and reslicing PET images. *J Comput Assist Tomogr*. 1992;14:620-633.
18. Woods RP, Mazziotta JC, Cherry SR. MRI-PET registration with automated algorithm. *J Comput Assist Tomogr*. 1993;17:536-46.
19. Wells WM III, Viola P, Atsumi H, Nakajima S, Kikinis R. Multi-modal volume registration by maximization of mutual information. *Med Image Analys*. 1996;1:35-51.
20. Robb RA, Hanson DP, Karwoski RA, et al. *AVW Reference Manual*. Technical Report. Rochester, MN: Mayo Foundation; 1998.
21. O'Brien TJ, Zupanc ML, Mullan BP, et al. The practical utility of performing peri-ictal SPECT in the evaluation of children with partial epilepsy. *Pediatr Neurology*. 1998;19:15-22.